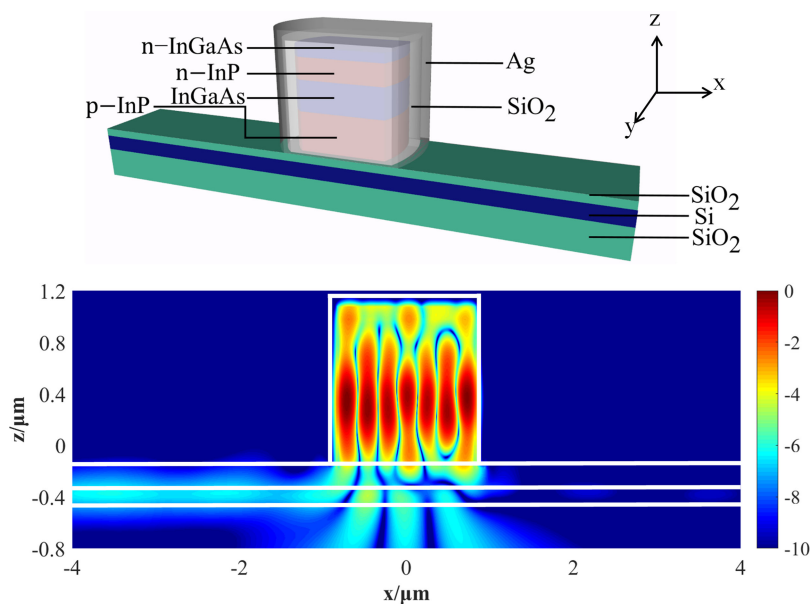


Design and Analysis of Asymmetric Capsule-Shaped Metallic Cavities for Unidirectional Waveguide Coupling




Volume 12, Number 6, December 2020

Baifu Zhang
Haifeng Hu
Hao Wang
Cheng Han
Zhe Shen
Ji Xu
Ming Sun
Li Li



DOI: 10.1109/JPHOT.2020.3033548

Design and Analysis of Asymmetric Capsule-Shaped Metallic Cavities for Unidirectional Waveguide Coupling

Baifu Zhang ¹, Haifeng Hu,¹ Hao Wang,¹ Cheng Han,¹
Zhe Shen ¹, Ji Xu,² Ming Sun,¹ and Li Li ¹

¹School of Electronic and Optical Engineering, Nanjing University of Science and Technology, Nanjing 210094, China

²College of Electronic and Optical Engineering & College of Microelectronics, Nanjing University of Posts and Telecommunications, Nanjing 210023, China

DOI:10.1109/JPHOT.2020.3033548

This work is licensed under a Creative Commons Attribution-NonCommercial-NoDerivatives 4.0 License. For more information, see <https://creativecommons.org/licenses/by-nc-nd/4.0/>

Manuscript received September 6, 2020; revised October 17, 2020; accepted October 20, 2020. Date of publication October 26, 2020; date of current version November 16, 2020. This work was supported in part by the NSAF (No. U1830123), in part by the National Natural Science Foundation of China under Grants 61627802, 61604073, 61805119 and 11404170, in part by the Natural Science Foundation of Jiangsu Province (BK20160839 and BK20180469), and in part by the Scientific Research Project of Nanjing University of Posts and Telecommunications (NY219045). (Baifu Zhang and Haifeng Hu are co-first authors.) Corresponding author: Baifu Zhang (e-mail: zhangbf@njust.edu.cn).

Abstract: We propose and numerically investigate a novel asymmetric capsule-shaped metallic cavity (ACMC) structure for unidirectional waveguide coupling. By introducing cylindrical facets at cavity ends with different radius, asymmetric resonant mode is confined inside the cavity so that the evanescent energy can be unevenly coupled into the two directions of the waveguide underneath the cavity. We conduct three-dimensional finite-difference time-domain simulations and demonstrate the effectiveness of the proposed ACMC-based unidirectional waveguide coupling. Besides, by modifying suitable geometry of the proposed structure, the extinction ratio and coupling efficiencies of both directions of the waveguide can be flexibly designed, resulting in unequal coupling of optical energy. In addition, the dependence of the waveguide-coupling properties on ACMC geometry is also numerically investigated in this paper.

Index Terms: Semiconductor lasers, Waveguides, Plasmonics.

1. Introduction

In last decade, a variety of metallic semiconductor cavity lasers has been proposed and studied for their promising applications, such as photonic integrated circuits (PICs), on-chip optical interconnection, optical communication, and so on [1]–[5]. Compared with the traditional waveguide-coupling scheme of semiconductor lasers, the optical energy inside the metallic cavity laser is generally coupled out through the waveguide underneath the bottom of the resonant cavity, where is free of metallic cladding [6]–[9]. Generally, increasing the coupling energy of the laser waveguide is of importance from practice point of view, but it contributes to higher radiation loss and thus lowers down quality (Q) factor of the metallic semiconductor cavity [6], [7]. To overcome this difficulty, various studies are conducted.

One method to solve this dilemma is focused on optimization of the cavity design and fabrication, in order to reduce cavity loss and enhance the laser performance. For example, improving the

fabrication technique [10], [11] and engineering the thermal effect of the metallic nanocavity [12]–[13] are two important issues for improving metallic semiconductor lasers, which have been demonstrated experimentally. Besides, optimizing the geometry of the cavity structure for a low-loss resonant mode can also increase the Q value effectively. For example, capsule-shaped cavity (CSC) structure [14]–[16] and Gaussian-shaped cavity (GSC) structure [17], which take advantage of Gaussian-like mode by introducing cylindrical facets to conventional metallic cavity, are proposed to confine the resonant mode tightly in the center of cavity with reduced metallic losses.

Another solution to the dilemma is focused on optimization of the waveguide structure and coupling scheme. Among the current metallic semiconductor cavity lasers, there are two main types of cavity structures including cylindrical cavity based on whispering-gallery mode [18]–[20] and rectangular cross-section cavity based on Fabry-Perot mode [21]–[22]. At present, the scheme of waveguide coupling from above types of metallic semiconductor lasers is mainly to embed the waveguide structure in the substrate layer [6]–[9], which couples the evanescent field of the resonance mode from the cavity into the waveguide. And by optimizing the geometric structure and spatial position of the waveguide, the coupling efficiency can be increased effectively. In general cases, due to the symmetry of the cavity and waveguide, the energy coupled from the cavity transmits to both directions of the waveguide evenly [6]. Therefore, unidirectional waveguide-coupling output is limited. To achieve unidirectional output, one reported method is to construct the waveguide only at one end of the cavity [7], [8]. However, this asymmetric waveguide structure limits the potential applications of the lasers, such as signal conversion and modulation.

In this paper, we propose a novel scheme of unidirectional waveguide coupling by designing asymmetric capsule-shaped metallic cavity (ACMC) with symmetric coupling waveguide structure. By optimizing the reflection facets of the cavity with different radius of curvature, the asymmetric Gaussian-like mode is resonant inside the cavity. As a result, the optical energy of the resonant mode can be coupled from the cavity into symmetry waveguide unidirectionally. We numerically demonstrate that the extinction ratio of the coupling efficiencies of two waveguide directions can reach as high as 17.3 at 1.55 μm wavelength range, indicating a unidirectional waveguide coupling. Moreover, the ratio of coupling efficiency on two sides of the waveguide can be modulated flexibly by designing suitable curvature of the facets. The proposed ACMC laser and its waveguide coupling scheme can be widely used in applications such as PICs, on-chip optical interconnects and so on.

2. Schematic and Design

The schematic of the proposed ACMC structure for unidirectional waveguide coupling is shown in Fig. 1. The two reflection facets of the ACMC are designed with different radius of curvature, shown in Fig. 1(c). The epitaxial structure of the ACMC consists of a 300-nm-thick InGaAs active layer sandwiched by the upper (500 nm thick) and the lower InP claddings, shown in Fig. 1(a). A 100-nm-thick n-doped InGaAs is used as a contact layer on top. The sidewalls of the mesa are covered by a 30-nm-thick SiO_2 layer to prevent the short circuit. The entire cavity structure is capped by 100-nm-thick silver, which also acts as the n-side contact from the top. The silver clad is much thicker than the skin depth at the investigated wavelength around 1.55 μm in this work [23], [24]. The substrate of the ACMC is embed with a waveguide structure, which consists of a core layer of Si sandwiched by the upper and lower claddings of SiO_2 respectively, shown in Fig. 1(b).

In this work, the waveguide coupling properties of the proposed structure are numerically studied by three-dimensional (3D) finite-difference time-domain (FDTD) simulation using the Lumerical FDTD solution-based commercial software package. The refractive indices of the materials InP, InGaAs, n-InGaAs, Si and SiO_2 are set to be 3.17, 3.53, 3.6, 3.42 and 1.45, respectively, and the permittivity of silver is fitted by Drude-Lorentzian model to experimental values [24], [25]. Perfectly matched layers (PML) are used on the boundaries of the computation area to absorb the reflective waves. The mesh size of cavity area (area A) is set to 5 nm and other area (area B) are covered by a non-uniform gradient mesh, shown in Fig. 1(d), where the mesh size is not larger than 12 nm, guaranteeing good convergence and rapid calculation time in our simulations.

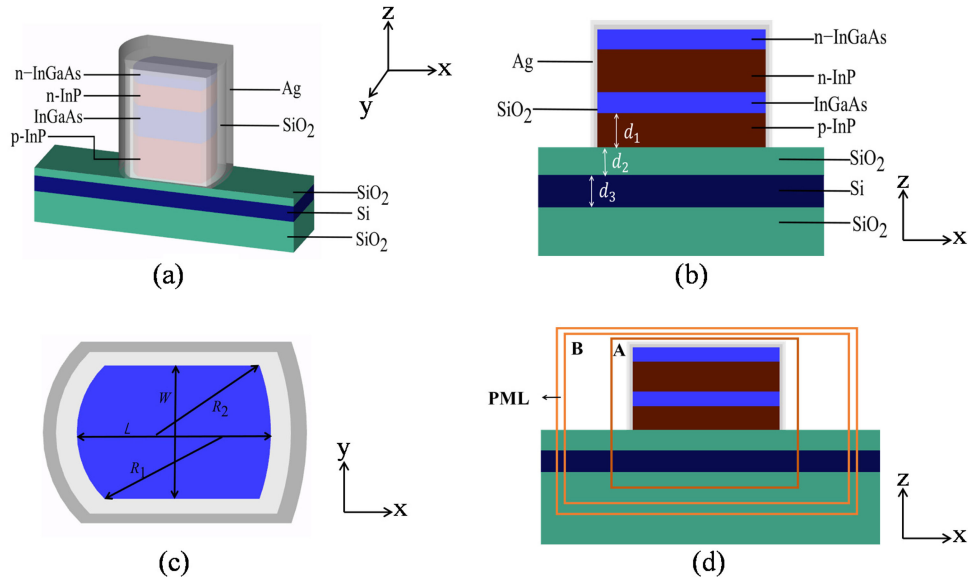


Fig. 1. ACMC structure for unidirectional waveguide coupling. (a) 3D view; (b) side view; (c) top view; (d) side view with simulation settings.

The waveguide coupling efficiency can be estimated as following [6], [7]:

$$\eta = \frac{P_C}{P_{total}} \times 100\% \quad (1)$$

where P_{total} is the total energy radiated from the proposed structure, and P_C is the energy output at the both ends of the waveguide. P_C can be expressed as $P_C = P_L + P_R$, where P_L and P_R are the energy output at the left and right end of the waveguide, respectively.

To characterize the properties of unidirectional waveguide coupling of the ACMC-based structure, we define the extinction ratio r_e as the ratio of coupling efficiency at both ends of the waveguide, which can be expressed by following formula:

$$r_e = \frac{\eta_L}{\eta_R} \quad (2)$$

$$\eta_L = \frac{P_L}{P_{total}} \times 100\% \quad (3)$$

$$\eta_R = \frac{P_R}{P_{total}} \times 100\% \quad (4)$$

Where η_L and η_R are the coupling efficiencies of the left and right side of the waveguide respectively. By calculating the waveguide coupling efficiency and the extinction ratio of different cavity structure, we numerically demonstrate the energy from cavity is unidirectionally coupled into symmetry waveguide, which will be discussed in detail in next section.

3. Results and Discussion

3.1 Symmetric CSC Waveguide Coupling

We conduct 3D FDTD simulations with excitation of an internal dipole source to investigate the proposed unidirectional waveguide coupling scheme of ACMC structure. To begin with, we first investigate the waveguide coupling properties of the conventional symmetric CSC structure for comparison. Note that the symmetric CSC structure can be regarded as a special case of the

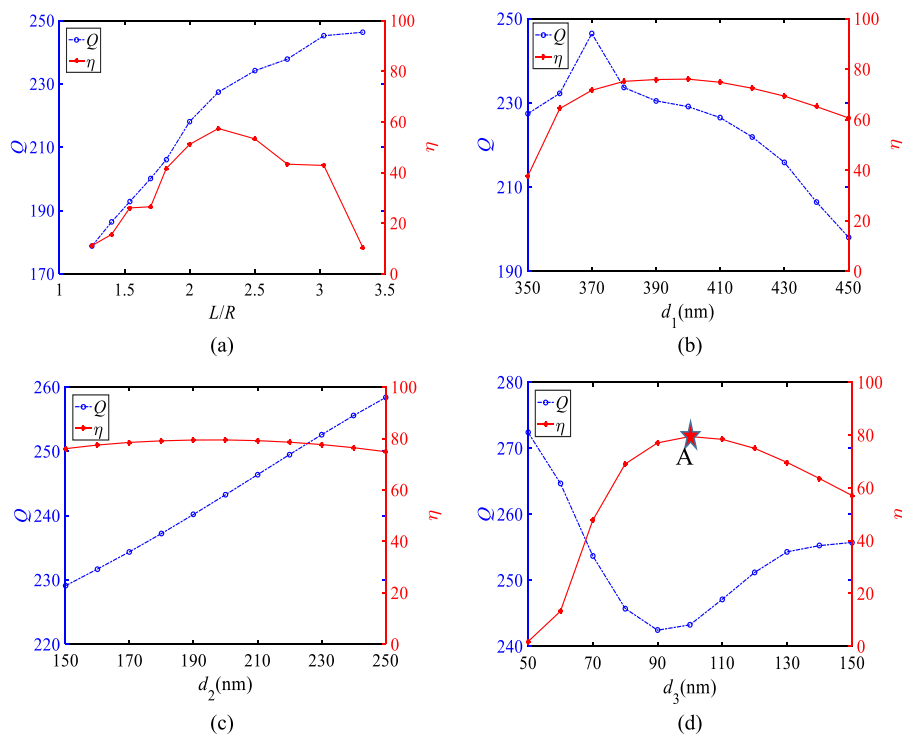


Fig. 2. Cavity Q factor of the symmetric CSC and waveguide coupling efficiency η as functions of L/R (a), the thickness d_1 of lower cladding of the cavity (b), the thickness d_2 of upper cladding of waveguide (c), and the thickness d_3 of Si waveguide core (d).

ACMC structure in Fig. 1, with the condition $R_1 = R_2 = R$. The CSC and ACMC structures are Fabry-Perot cavities, indicating that the resonant wavelength is sensitive to the cavity length L . We elaborately select the length L and width W of the cavity shown in the Fig. 1(c) to be 1620 nm and 800 nm, respectively, which guarantees the resonant mode within 1.53–1.57 μm wavelength range in all the simulations in this work. To study the dependence of the Q value and the waveguide coupling efficiency η on the cavity geometry, we first investigate the radius of curvature R of the cavity with fixed parameters $d_1 = 350$ nm, $d_2 = 150$ nm and $d_3 = 100$ nm. Fig. 2(a) plots the Q and η of the CSC structure as a function of R , where L/R represents the ratio of the cavity length to the radius of curvature. From Fig. 2(a), we can see that the coupling efficiency increases with the radius of curvature and takes maximum at $L/R = 2.22$, and then shows a diminishing trend in general. However, when $L/R \leq 1.7$ the η is reduced drastically due to the dominant vertical radiation loss.

With the optimal radius of curvature ($L/R_1 = 2.22$) and fixed parameters $d_2 = 150$ nm and $d_3 = 100$ nm, the Q factor and waveguide coupling efficiency as a function of the thickness of the lower InP cladding of the cavity are then numerically studied and plotted in Fig. 2(b). The η firstly increases with d_1 until taking maximum value of 76% at $d_1 = 400$ nm, then it shows a slowly decreasing trend. While the Q factor shows a similar trend to that of the η , but takes maximum value at $d_1 = 370$ nm, which means that the optimal cavity structure with lowest radiation loss does not contribute to an optimal coupling efficiency.

Next, we sweep the thicknesses of upper cladding and core layers of the waveguide with fixed $L/R_1 = 2.22$ and $d_1 = 400$ nm, respectively, to study the dependence of Q value and the η on d_2 and d_3 , which are calculated and plotted in Figs. 2(c) and (d). It should be mentioned that the thickness of Si waveguide core is selected less than 150 nm to guarantee single mode coupling [6], for example, d_3 is fixed to be 100 nm in Fig. 2(c). From Fig. 2(c) we can see that the η is not as sensitive to the variance of d_2 as Q value, because the later one can be increased with lower

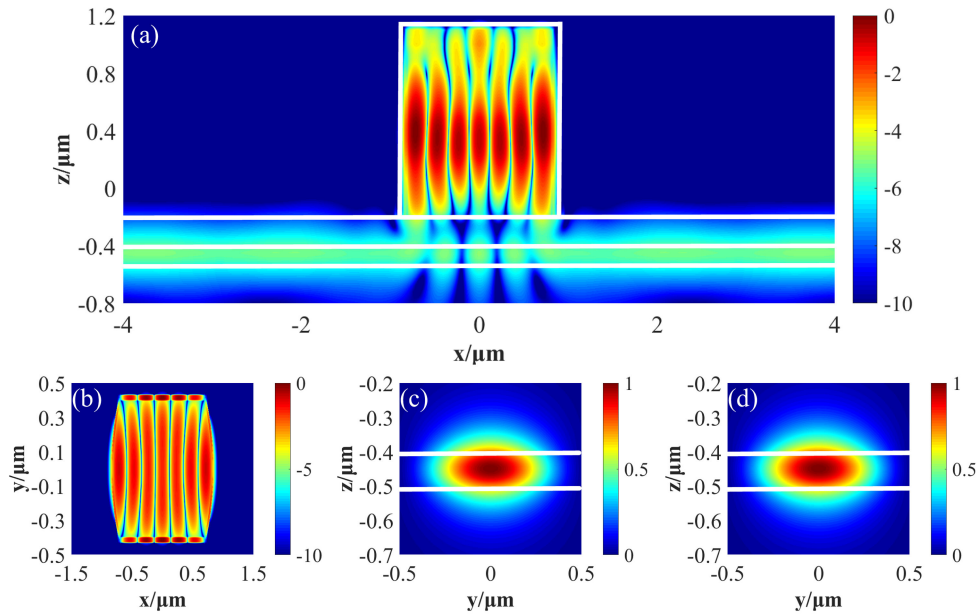


Fig. 3. Normalized electric field intensity distributions $|E|^2$ of symmetric CSC structure in xz plane (a) and xy plane (b) crossing the center of the cavity (in logarithm scale), and in yz planes at the left end (c) and right end (d) of the waveguide, respectively.

radiation loss when the d_2 becomes thicker. While both the Q value and η depend on d_3 more heavily and take nearly opposite trend to each other. For example, at the point $d_3 = 100$ nm in Fig. 2(d) where d_2 is fixed to 200 nm, the η reaches the peak value of 79.5% but the Q factor takes minimum value of 243.3, indicating the most effective coupling of the waveguide structure and the highest external radiation of the cavity. The electric field intensity distribution of the resonant mode corresponding to the point A in Fig. 2(d) is depicted in Fig. 3. We can see that the energy coupled from the cavity propagates to both ends of the waveguide evenly.

3.2 ACMC Waveguide Coupling

The symmetric waveguide coupling investigated above contributes to identical energy output through both ends of the waveguide. To realize unidirectional waveguide coupling, we design different radius of curvature at the two ends of the resonant cavity, in order to introduce symmetric-breaking structure in length scale so that asymmetric coupling is achieved. For simplicity, we first fix R_1 value as $L/R_1 = 2.22$, and then sweep R_2 to study the asymmetric structure. Fig. 4 plots the Q value, extinction ratio r_e and coupling efficiencies as functions of L/R_2 , where we can see that the r_e decreases with L/R_2 . When L/R_2 is 2.22, the cavity is symmetric and consequently the r_e is 1. Thus, the electric field intensity distribution is identical and the energy output at both ends is equal. While $L/R_2 = 0$ corresponds to a rectangular facet at the right end of the cavity, and extinction ratio of this structure takes maximum value of 13.5, indicating that the energy of left end is much larger than that of right end of the waveguide. However, the leakage loss of the asymmetric structure with $L/R_2 = 0$ and $L/R_1 = 2.22$ is so high that its total coupling efficiency is much smaller than that of the symmetric structure, shown in Fig. 2.

Next, we fix the radius of curvature R_2 to be infinite large ($L/R_2 = 0$), and then optimize the alternative radius of curvature R_1 to get flexible energy distribution of the asymmetric waveguide coupling process, shown in Fig. 5(a). It shows that the extinction ratio r_e can achieve above 10 within the range of L/R_1 from 2.22 to 3.70, indicating a good fabrication tolerance of the cavity geometry. Further, the influence of the thicknesses d_1 , d_2 and d_3 is also numerically investigated,

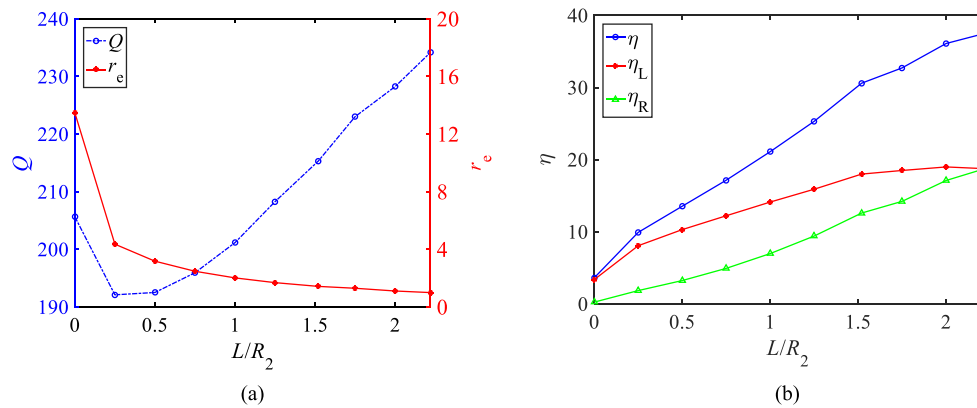


Fig. 4. Cavity Q factor and extinction ratio r_e (a), and coupling efficiencies (b) of the ACMC waveguide coupling structure as a function of L/R_2 . Note that the fixed parameters are set to be $L/R_1 = 2.22$, $d_1 = 350$ nm, $d_2 = 150$ nm, and $d_3 = 100$ nm in the simulations.

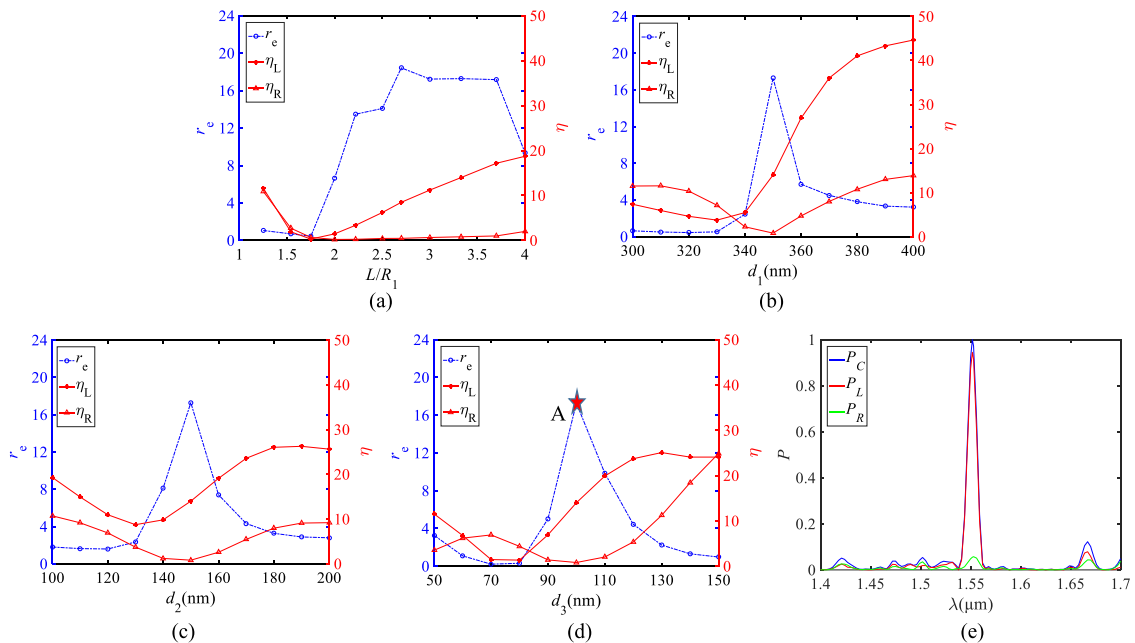


Fig. 5. Extinction ratio r_e and coupling efficiencies of ACMC structures as functions of L/R_1 (a), the thickness d_1 of lower cladding of the cavity (b), the thickness d_2 of upper cladding of waveguide (c), and the thickness d_3 of Si waveguide core (d). And (e) plots the output power P_C , P_L and P_R of the ACMC structure as a function of wavelength, corresponding to the point A in (d). Note that the fixed parameters are set to be $L/R_2 = 0$, $L/R_1 = 3.33$, $d_1 = 350$ nm, $d_2 = 150$ nm and $d_3 = 100$ nm in the corresponding simulations.

shown in Figs. 5(b)-(d). Note that the extinction ratio and coupling efficiency are not optimal at the same structure so that suitable geometry needs to be elaborately designed according to the concrete applications. For example, by tuning geometric parameters, a structure with high r_e up to 17.3 and moderate coupling efficiency of 14.8% can be realized, corresponding to the point A in Fig. 5(d). Besides, we investigate the output power P at each waveguide end of the ACMC structure corresponding to the point A in Fig. 5(d), as a function of wavelength, shown in Fig. 5(e). All the data in Fig. 5(e) is normalized by the total output power P_C at the resonant wavelength of 1551.8 nm. It shows that the output power is dominant at the resonant wavelength.

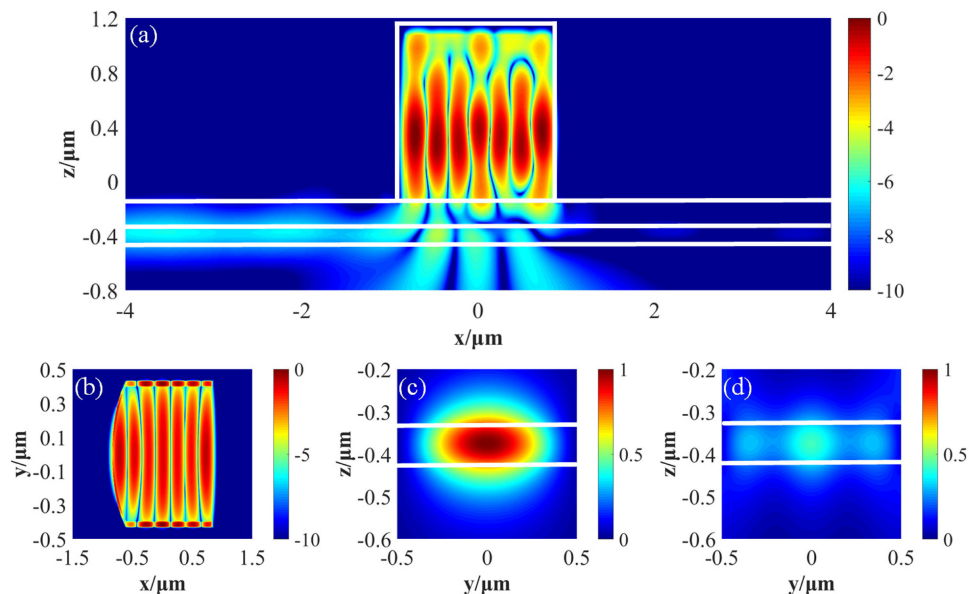


Fig. 6. Normalized electric field intensity distributions $|E|^2$ of ACMC structure in xz plane (a) and xy plane (b) crossing the center of the cavity (in logarithm scale), and in yz planes at the left end (c) and right end (d) of the waveguide, respectively.

At last, Fig. 6 shows the electric field intensity distribution of the resonant mode corresponding to the point A in Fig. 5(d). Fig. 6(a) depicts the optical energy distribution inside the waveguide, indicating unidirectional coupling clearly. And the normalized electric intensity distributions in the left and right cross-sections at waveguide ends are shown in Figs. 6(c) and (d) respectively. Consistent with Fig. 6(a), we can see that the energy of waveguide mode in the left side overwhelms that of the right side. We ascribe this unidirectional waveguide coupling to the asymmetric resonant cavity mode formed by ACMC structure, shown in Fig. 6(b). Unlike conventional method of asymmetric waveguide structure, we demonstrate unidirectional waveguide coupling by an asymmetric cavity structure but with symmetric waveguide, allowing flexible applications for unequal couplings of two waveguide sides.

4. Conclusion

In conclusion, we have proposed and numerically studied a novel ACMC structure with different curved facets for unidirectional waveguide coupling of semiconductor lasers. Since the asymmetric resonant mode is formed by the ACMC structure inside the cavity, its evanescent energy can be unevenly coupled into two directions of the waveguide structure underneath the cavity. A variety of properties of the ACMC-based waveguide coupling, such as resonant mode and waveguide mode distribution, cavity Q factor, coupling efficiency, extinction ratio, etc., are numerically studied by 3D full wave FDTD simulations. By modifying the geometry of the proposed structure, extinction ratio of the coupling efficiencies at both waveguide ends, up to 17.3, is numerically achieved, demonstrating the effectiveness of the ACMC-based unidirectional waveguide coupling. Besides, our study also shows that, by elaborately tuning the ACMC topology, the extinction ratio and coupling efficiencies of both directions of the waveguide can be flexibly designed, taking the advantage of allowing unequal coupling of optical energy. The proposed structure can be one of promising strategies in realizing flexible waveguide coupling of semiconductor nanolasers for applications in PICs, on-chip interconnects, optical communications and so on.

References

- [1] D. A. B. Miller, "Attojoule optoelectronics for low-energy information processing and communications," *J. Lightw. Technol.*, vol. 35, no. 3, pp. 346–396, Feb. 2017.
- [2] M. Smit, J. V. D. Tol, and M. Hill, "Moore's law in photonics," *Laser Photon. Rev.*, vol. 6, no. 1, pp. 1–13, Jan. 2012.
- [3] K. C. Y. Huang, M.-K. Seo, T. Sarmiento, Y. Huo, J. S. Harris, and M. L. Brongersma, "Electrically driven subwavelength optical nanocircuits," *Nat. Photon.*, vol. 8, pp. 244–249, Feb. 2014.
- [4] M. T. Hill, "Electrically pumped metallic and plasmonic nanolasers," *Chin. Phys. B.*, vol. 27, no. 11, 2018, Art. no. 114210.
- [5] R. M. Ma and R. F. Oulton, "Applications of nanolasers," *Nat. Nanotechnol.*, vol. 14, pp. 12–22, Jan. 2019.
- [6] M. K. Kim, A. M. Lakhani, and M. C. Wu, "Efficient waveguide-coupling of metal-clad nanolaser cavities," *Opt. Express*, vol. 19, no. 23, pp. 23504–23512, Nov. 2014.
- [7] H. Long *et al.*, "Investigation of high efficiency unidirectional emission from metal coated nanocylinder cavities," *J. Lightw. Technol.*, vol. 32, no. 18, pp. 3192–3198, Jul. 2014.
- [8] K. Feng *et al.*, "Waveguide-coupled metal-clad cavity with integrated feedback stub," *Jpn. J. Appl. Phys.*, vol. 56, no. 8, Jul. 2017, Art. no. 082201.
- [9] V. D. Calzadilla *et al.*, "Waveguide-coupled nanopillar metal-cavity light-emitting diodes on silicon," *Nat. Commun.*, vol. 8, Feb. 2017, Art. no. 14323.
- [10] K. Ding and C. Z. Ning, "Fabrication challenges of electrical injection metallic cavity semiconductor nanolasers," *Semicond. Sci. Technol.*, vol. 28, Jun. 2013, Art. no. 12.
- [11] Ding *et al.*, "Record performance of electrical injection sub-wavelength metallic-cavity semiconductor lasers at room temperature," *Opt. Express*, vol. 21, no. 4, pp. 4728–4733, Feb. 2013.
- [12] J. S. T. Smalley, Q. Gu, and Y. Fainman, "Temperature dependence of the spontaneous emission factor in subwavelength semiconductor lasers," *IEEE J. Quantum Electron.*, vol. 50, no. 3, pp. 175–185, Mar. 2014.
- [13] Q. Gu, J. S. T. Smalley, J. Shane, Bondarenko, and Y. Fainman, "Temperature effects in metal-clad semiconductor nanolasers," *Nanophotonics*, vol. 4, no. 1, pp. 26–43, Apr. 2015.
- [14] B. Zhang *et al.*, "Proposal and numerical study on capsule-shaped nanometallic semiconductor lasers," *Jpn. J. Appl. Phys.*, vol. 53, no. 11, Jan. 2015, Art. no. 112703.
- [15] B. Zhang, K. Chieda, T. Okimoto, T. Tanemura, and Y. Nakano, "Q factor improvement by capsule-shaped metallic cavity structure for subwavelength lasers," *Phys. Status Solidi A*, vol. 213, no. 4, pp. 965–969, Apr. 2016.
- [16] Y. Xiao, R. J. E. Taylor, C. Yu, K. Feng, T. Tanemura, and Y. Nakano, "Room-temperature capsule-shaped wavelength scale metal-clad laser with enhanced side mode suppression," *Appl. Phys. Lett.*, vol. 111, no. 8, Aug. 2017, Art. no. 081107.
- [17] B. Zhang *et al.*, "Design and numerical study of semiconductor nanolaser with Gaussian-shaped metallic cavity," *IEEE Photon. J.*, vol. 213, no. 4, Nov. 2018, Art. no. 4502110.
- [18] W. E. Hayenga *et al.*, "Metallic coaxial nanolasers," *Adv. Phys. X*, vol. 1, no. 2, pp. 262–275, May 2016.
- [19] M. Khajavikhan *et al.*, "Thresholdless nanoscale coaxial lasers," *Nature*, vol. 482, no. 7384, pp. 204–207, Feb. 2012.
- [20] C.-C. Guo, J.-L. Xiao, Y.-D. Yang, and Y.-Z. Huang, "Mode characteristics of subwavelength aluminum/silica-coated InAlGaAs/InP circular nanolasers," *J. Opt. Soc. Amer. B*, vol. 31, no. 4, pp. 865–872, Apr. 2014.
- [21] M. T. Hill *et al.*, "Lasing in metal-insulator-metal sub-wavelength plasmonic waveguides," *Opt. Express*, vol. 17, no. 13, pp. 11107–11112, 2009.
- [22] K. Ding *et al.*, "Room-temperature continuous wave lasing in deep-subwavelength metallic cavities under electrical injection," *Phys. Rev. B*, vol. 85, no. 4, Jan. 2012, Art. no. 041301.
- [23] M. Fox, *Optical Properties of Solids*. 1st ed. New York, NY, USA: Oxford Univ. Press, 2001.
- [24] E. D. Palik, *Handbook of Optical Constants of Solids*. New York, NY, USA: Academic Press, 1985.
- [25] A. Taflove and S. C. Hagness, *Computational Electrodynamics: The Finite-Difference Time-Domain Method*. 3rd ed. Norwood, MA, USA: Artech House, 2005.